

Discovery and SAR of Novel Disubstituted Quinazolines as Dual PI3K α /mTOR Inhibitors Targeting Breast Cancer

Aisha A. K. Al-Ashrawy,* Khaled M. Elokely, Oscar Perez-Leal, Mario Rico, John Gordon, George Mateo, Abdelsattar M. Omar, Magid Abou-Gharbia, and Wayne E. Childers, Jr.*



Cite This: <https://dx.doi.org/10.1021/acsmchemlett.0c00289>



Read Online

ACCESS |



Metrics & More



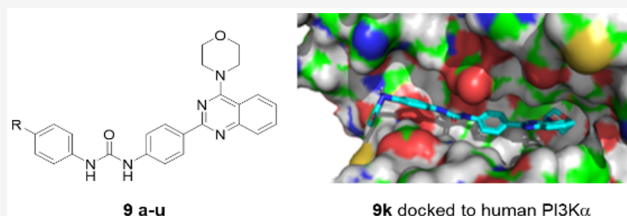
Article Recommendations



Supporting Information

ABSTRACT: The dual PI3K α /mTOR inhibitors represent a promising molecularly targeted therapy for cancer. Here, we documented the discovery of new 2,4-disubstituted quinazoline analogs as potent PI3K α /mTOR inhibitors. Our structure based chemistry endeavor yielded six excellent compounds **9e**, **9f**, **9g**, **9k**, **9m**, and **9o** with single/double digit nanomolar IC₅₀ values against both enzymes and acceptable aqueous solubility and stability to oxidative metabolism. One of those analogs, **9m**, possessed a sulfonamide substituent, which has not been described for this chemical scaffold before. The short direct synthetic routes, structure–activity relationship, *in vitro* 2D cell culture viability assays against normal fibroblasts and 3 breast cancer cell lines, and *in vitro* 3D culture viability assay against MCF7 cells for this series are described.

KEYWORDS: 4-Morpholinoquinazolines, PI3K α , mammalian target of rapamycin, mTOR, dual inhibitors, breast cancer cell lines



The human PI3K/Akt/mTOR signaling pathway is implicated in vital processes such as cell proliferation, survival, and metabolism. This central pathway receives growth signals and then propagates them through a series of phosphorylations and dephosphorylations of downstream effectors.¹ Phosphatidylinositol-3-kinases (PI3Ks) are lipid kinases which catalyze the phosphorylation of phosphatidylinositol(4,5)-biphosphate (PIP2) to phosphatidylinositol(3,4,5)-triphosphate (PIP3). This secondary messenger is the master key in signal transfer through the activation of protein kinase B (Akt) and other downregulators such as mammalian target of rapamycin (mTOR). According to structural features and substrate specificity, PI3Ks are divided into four classes, I (subclassified as IA and IB), II, III, and IV. Class IV enzymes are also defined as phosphoinositide-3-kinase related protein kinases (PIKKs), and they share a conserved catalytic domain sequence to that of PI3Ks. PI3K α is an example of Class IA, while mTOR, a serine-threonine kinase, belongs to Class IV.^{2,3}

Dysfunction of the PI3K/Akt/mTOR signaling pathway has been implicated in many human cancers such as breast, ovarian, prostate, colorectal, and glioblastoma.^{4,5} Breast cancer is the most common cause of death among women. Approximately 12% of women may acquire breast cancer over the period of their lifetime (www.breastcancer.org). Generally, the pathological activation of this pathway is thought to be due to amplification of proto-oncogenes (e.g., PI3KCA, Akt), silencing of tumor suppressor genes (e.g., phosphatase and tensin homologue deleted on chromosome ten (PTEN):PIP3 phosphatase), and/or overexpression of

upstream regulator receptor tyrosine kinases (RTKs). Regardless of the mechanistic cause, the end result is tumorigenesis and angiogenesis.⁶

Oncology drug discovery for these cancers targets key nodes in this pathway to avoid the feedback of downstream effectors and to gain expected synergistic suppression.^{7–9} Upregulation of the PI3K pathway is a major mechanism of resistance to many molecularly targeted cancer therapeutics.¹⁰ Therefore, the design of small molecule ATP competitive dual PI3K α /mTOR inhibitors is an appealing approach which has been underserved to date as there is only one approved drug on the market. There are, however, some advanced candidates in different phases of development (Figure 1). Pfizer is currently performing Phase II clinical trials on gedatosisib (PKI-587, **1**), a potent selective triazine derivative, for the treatment of breast cancer and acute myeloid leukemia.¹¹ Sanofi-Aventis is examining voxalisib (XL-765, **2**) in phase I studies for the oral treatment of lymphoma and solid tumors.^{12,13} PI-103 (**3**) was the first quinazoline analog reported to display PI3K α inhibitory activity.¹⁴ However, it did not enter clinical trials because of its rapid *in vivo* metabolism.¹⁵ A trisubstituted quinazoline derivative (**4**), exhibited a potent dual PI3K α /mTOR inhibition with good antiproliferative activity against

Received: May 28, 2020

Accepted: October 6, 2020

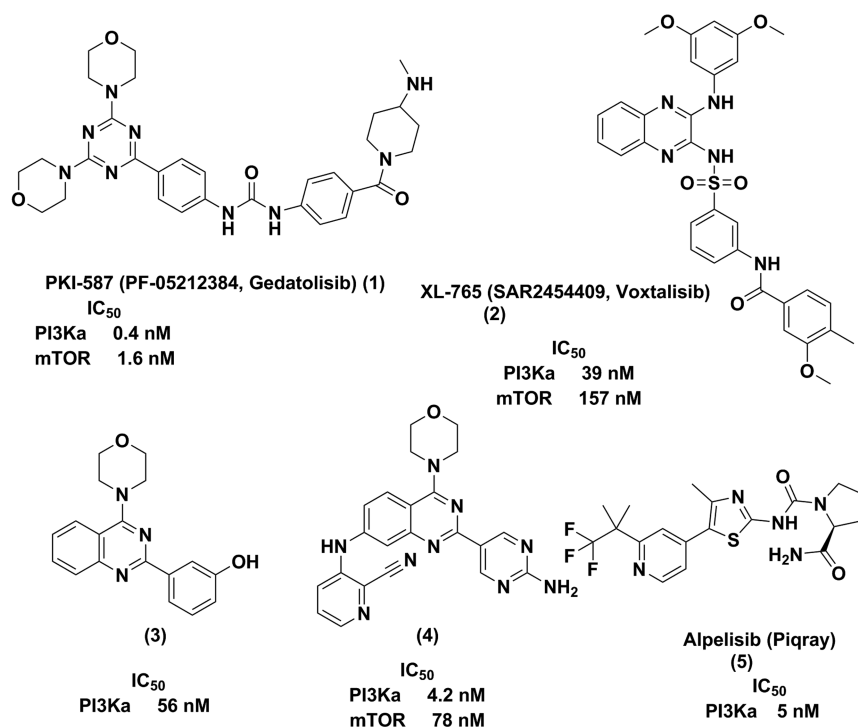


Figure 1. Quinazolines as dual PI3K α /mTOR inhibitors.

the U937 cell line.¹⁶ And in 2019, the FDA approved the first α -subtype specific PI3K inhibitor from Novartis, alpelisib (Piqray, 5), for use in combination with endocrine therapy in postmenopausal women with PI3K α -mediated advanced breast cancer.¹⁷

In 2017, we reported a series of pyridopyrimidine-based ATP-competitive dual PI3K α /mTOR inhibitors.¹⁸ Our disubstituted analogs demonstrated potent inhibitory activity against both enzymes with selectivity toward PI3K α over mTOR. Compound A (Figure 2) was exemplified with PI3K α

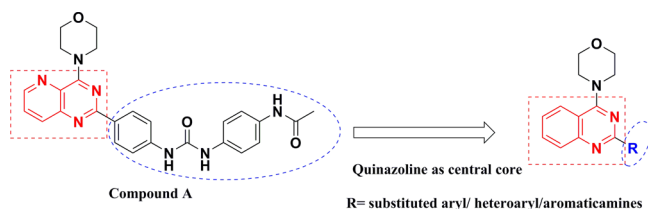


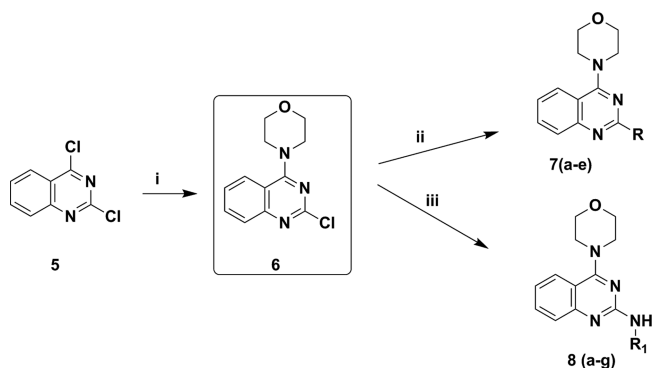
Figure 2. Initial strategy for designing 2-substituted-4-morpholinoquinazolines.

IC_{50} = 0.5 nM, mTOR IC_{50} = 104 nM, and excellent antiproliferative activity against MCF7 with IC_{50} = 170 nM. Docking studies with compound A and the crystal structures of PI3K α and mTOR revealed structural features of the C2 substituents that impacted on binding to both enzymes and imparted selectivity for PI3K α over mTOR. In this paper we report our efforts to extrapolate those structural revelations to the quinazoline scaffold.

Our first strategy was to simplify the structure by replacing the diaryl urea moiety with substituted aryl, heteroaryl, or substituted aromatic amines as depicted in Figure 2. We wished to explore whether these substituents would mimic the diaryl urea moiety in both the binding affinity and inhibitory activity toward the two enzymes.

The syntheses of these compounds were accomplished following the 2-step direct synthetic route shown in Scheme 1.

Scheme 1. Synthesis of 4-Morpholinoquinazoline Derivatives C2 Substituted by Aryl, Heteroaryl, and Substituted Aromatic Amines^a



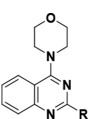
^aReagents and conditions: (i) morpholine, triethyl amine, dry THF, stir 3 h, rt; (ii) (Het)ArB(OH)₂ or pinacol ester, K₂CO₃, Pd(PPh₃)₄, DME, 150 °C, 20 min microwave; (iii) aromatic amines, NaI, DMA, 160 °C, 15 min microwave.

Nucleophilic displacement of the 4-chloro group on the commercially available 2,4-dichloroquinazoline with morpholine under dry basic conditions gave intermediate 6. Under microwave irradiation, this intermediate was coupled with either boronic acids or pinacol esters under Suzuki–Miyaura conditions to form compounds 7a–e or treated with substituted anilines to yield 8a–g (Supporting Information).

The HotSpot radioisotope filter binding assay was used to assess the *in vitro* enzymatic inhibitory activity for the novel quinazoline derivatives at 10 μ M concentration in the presence of 10 μ M ATP and using PI-103 as reference (Table S2).

Inhibitory activity against human PI3K α was assessed by measuring the conversion of phosphatidylinositol(4,5)-biphosphate to phosphatidylinositol(3,4,5)-triphosphate. The ability to inhibit human mTOR was assessed by measuring the phosphorylation of factor 4E-binding protein1 (4EBP1). In this series, all the compounds showed a moderate inhibitory activity at this concentration. Consequently, the best three compounds 7d, 8d, and 8e were subjected to a concentration–response study to determine IC₅₀ values against both enzymes. Results are shown in Table 1 together with *in vitro* ADME

Table 1. Kinase Inhibitory Activity, Solubility, and Mouse Liver Microsomal Stability of 7d, 8d, and 8e



Entry	R-Group	Kinase Inhibition		Max. Aq. Sol (pH 7.4)	Microsomal Stability t _{1/2} (min)
		PI3K α IC ₅₀ (μ M)	mTOR IC ₅₀ (μ M)		
PI-103	NA	0.002	0.02	3.4	7.1
7d		8.8	1.8	86.8	2.1
8d		5.9	NA	22.7	44.9
8e		6.9	11.4	42.6	52

screening data measuring the maximum kinetic aqueous solubility in 2% DMSO/phosphate-buffered saline (pH = 7.4) and metabolic stability in mouse liver microsomes, expressed in t_{1/2} (min).

Unfortunately, the strategy of simplifying the structure yielded weak dual PI3K α /mTOR inhibitors with IC₅₀ values in the micromolar range. Representative data are shown in Table 1, and data for 7a–e and 8a–g are provided in Table S1. Maximum kinetic aqueous solubility for these analogs, in general, was better than that seen for PI-103 and t_{1/2} values in mouse liver microsomes ranged from 2.1 min to >60 min, with many analogs demonstrating superior stability to that seen with PI-103 (t_{1/2} = 7.1 min). The results obtained in the kinase inhibition assays highlighted the critical role of the phenylurea moiety in this series of derivatives for potent dual enzyme inhibition. Therefore, we reverted to our second optimization strategy in which we kept the urea moiety intact and substituted it with alkyl groups and aryl rings containing hydrogen bond donating or accepting functional groups to explore the structural requirements of the PI3K α and mTOR binding pockets as represented in Figure 3.

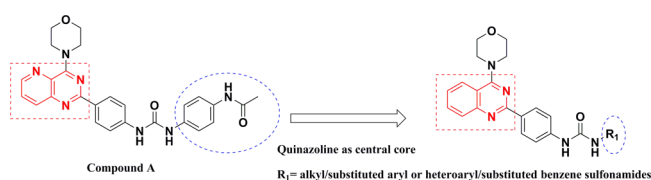
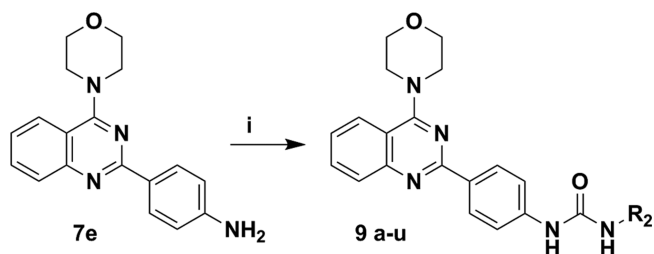


Figure 3. Second strategy for designing 4-morpholino-quinazoline urea derivatives.

The syntheses of these substituted ureas were achieved through the *in situ* conversion of 7e to the isocyanate by reaction with triphosgene under dry conditions followed by treatment with the appropriate amine/aniline to give 9a–u as presented in Scheme 2.

Scheme 2. Synthesis of 4-Morpholinoquinazoline–Urea Derivatives Substituted by Alkyl (9a,b), Substituted Phenyl (9c–l), and Substituted Benzenesulfonamides (9m–u)



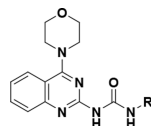
Of the 21 synthesized analogs, 16 afforded $\geq 90\%$ inhibition at 10 μ M concentration against both PI3K α and mTOR in the Hotspot radioisotope filter binding assay (Table S2). IC₅₀ values were determined for these 16 analogs (Table 2). The type and size of the substituent directly influenced the potencies for both enzymes. The newly synthesized derivatives possessed low to excellent aqueous solubility in 2% DMSO/phosphate buffered solution. Concerning the mouse microsomal metabolic stability, these new analogs demonstrated a range from moderate (e.g., t_{1/2} = 23.5 min for 9s) to excellent (many t_{1/2} value > 60 min) stability. Results of 9a–u are shown in Table 2.

Initial SAR studies revealed that the replacement of the phenyl urea ring with a short alkyl side chain such as methyl 9a or ethylalcohol 9b caused an increase in selectivity for mTOR over PI3K α by 2-fold to 3-fold. Substitution of the alkyl group with phenyl (9c) enhanced potency for PI3K α and reduced potency for mTOR, giving an analog that was 4-fold selective for PI3K α . Interestingly, incorporation of heteroatoms in that phenyl ring (9d) eliminated PI3K α selectivity (IC₅₀ for PI3K α and mTOR = 114 nM and 115 nM, respectively).

In order to probe the size and electronic nature of the binding pockets around the urea moiety, we prepared a series of analogs with hydrogen bonding substituents on the phenyl ring. These included hydroxymethyl in the para (9e) and meta (9f) positions as well as the para-hydroxyethyl derivative (9g). An increase in both PI3K α and mTOR inhibitory potency was realized with all three derivatives compared to the unsubstituted analog 9c, and the para-substitution pattern appeared to be better tolerated. All three analogs displayed selectivity for PI3K α over mTOR, especially 9g which was 40-fold selective. These results suggested the presence of a hydrogen bond acceptor near the para-position of the phenyl ring and the possibility that the binding pocket on PI3K α may be somewhat larger/longer than the pocket on mTOR.

Substituting structurally similarly sized groups with oxygen-containing hydrogen bond acceptor moieties in the para position (9h, 4-acetyl; 9i, 4-propanyl; 9j, 4-carboethoxy) caused a loss in potency for both enzymes. However, a significant increase in potency against PI3K α was realized when the strongly hydrogen bond accepting amide groups (-NHCO-, -CONH-) were inserted in the para position of the phenylurea ring (9k and 9l, PI3K α IC₅₀ = 0.7 nM and 2.5 nM,

Table 2. Kinase Inhibitory Activity, Aqueous Solubility, and Mouse Liver Microsomal Stability of 9a–u



Entry	R-Group	Kinase Inhibition		Max. Aq. Sol. (μM)	Mic. Stability $t_{1/2}$, min
		IC ₅₀ (nM) PI3K α	mTOR		
PI-103	N/A	2.0	20.0	3.4	7.1
9a	-CH ₃	186	61.2	192	8
9b		185	86.6	200	53.1
9c		12	504	8.1	> 60
9d		114	115	2.7	24.5
9e		2.4	58.8	14.3	> 60
9f		7.2	159	8.2	> 60
9g		1.41	52.2	5.9	38.2
9h		16.6	243	2	> 60
9i		77% [†]	73% [†]	4	> 60
9j		73% [†]	81% [†]	< 2	30.5

Entry	R-Group	Kinase Inhibition		Max. Aq. Sol. (μM)	Mic. Stability $t_{1/2}$, min
		IC ₅₀ (nM) PI3K α	mTOR		
9k		0.7	114	< 2	> 60
9l		2.5	59.1	< 2	> 60
9m		3.4	95.1	< 2	> 60
9n		6.2	204	6.9	60
9o		18.5	42	6.1	> 60
9p		26.1	83	3.1	> 60
9q		84% [†]	93.4	< 2	37.8
9r		83% [†]	37.4	13.6	> 60
9s		63% [†]	75% [†]	< 2	23.1
9t		54% [†]	60% [†]	< 2	> 60
9u		56% [†]	70% [†]	4.3	> 60

[†]Percent inhibition at a concentration of 10 μM .

respectively). Both compounds maintained reasonable potency against mTOR (IC₅₀ = 114 nM and 59.1 nM, respectively). However, the order of the atoms within the amide substituent had opposite effects, with the switch from the acetanilino structure in **9k** to the carboxamide structure in **9l** resulting in a loss of potency against PI3K α and an increase in potency against mTOR. Indeed, compound **9k** was the most potent PI3K α inhibitor of all the analogs prepared for this study and displayed the greatest selectivity for PI3K α over mTOR (154-fold) compared to other quanzolines within this series.

To further probe the PI3K α and mTOR binding sites for this series, we substituted the para-amide motif with sulfonamide moieties. Compared to the corresponding carboxamide derivative **9l**, the unsubstituted sulfonamide derivative **9m** retained similar inhibitory potency for PI3K α but lost some potency against mTOR. Contrary to the amides **9l** and **9k**, when the order of the atoms for the sulfonamide group in **9m** was reversed to give **9n**, a loss in both PI3K α and mTOR inhibitory potency was seen. Further derivatization of the sulfonamide motif present in **9m** resulted in several analogs that lost PI3K α potency but retained inhibitory potency for mTOR. These included the guanidinesulfonamide **9o**, the thiazolyl analog **9p**, the pyridinyl derivative **9q**, and especially the pyrimidinyl compound **9r**, which was the most potent mTOR inhibitor of the compounds prepared for this study with an mTOR IC₅₀ value = 37.4 nM. Either hydrogen bonding or the electronic nature of the ring appeared to play a

role in mTOR affinity as the corresponding phenyl sulfonamide **9s** and the electron-poor 2-fluorophenyl and 2,4-diphenyl derivatives **9t** and **9u**, respectively, also lost potency against mTOR activity compared to the heteroaryl analogs **9q** and **9r**. It should be noted that to our knowledge, this is the first time that the sulfonamide substituent has been examined as part of the SAR of this class of PI3K α /mTOR inhibitor.

Most of the urea analogs prepared for this study possessed low to moderate maximum kinetic aqueous solubility in 2% DMSO/phosphate buffered saline, although those solubilities were comparable to that seen with the standard PI-103. The exception to this trend was the alkyl analogs **9a** and **9b**, for which 192 μM and 200 μM solutions, respectively, were obtained. With the exception of methylurea derivative **9a**, all of the prepared analogs demonstrated superior stability to oxidative metabolism in mouse liver microsomes compared to PI-103. These data were not influenced by solubility limitations since the concentration of test compounds used in the microsomal stability assays was 1 μM .

To better understand our results, we performed docking studies of compounds **9k** (PI3K α -selective) and **9r** (mTOR-selective) with human PI3K α and mTOR using the published cocrystal structures of these compounds with human PI3K α (PDB 4L23)¹⁹ and mTOR (PDB 4JT6)²⁰ bound to PI-103. Binding modes were predicted using Glide SP. Hydrogen bond constraints were employed, followed by generalized energy

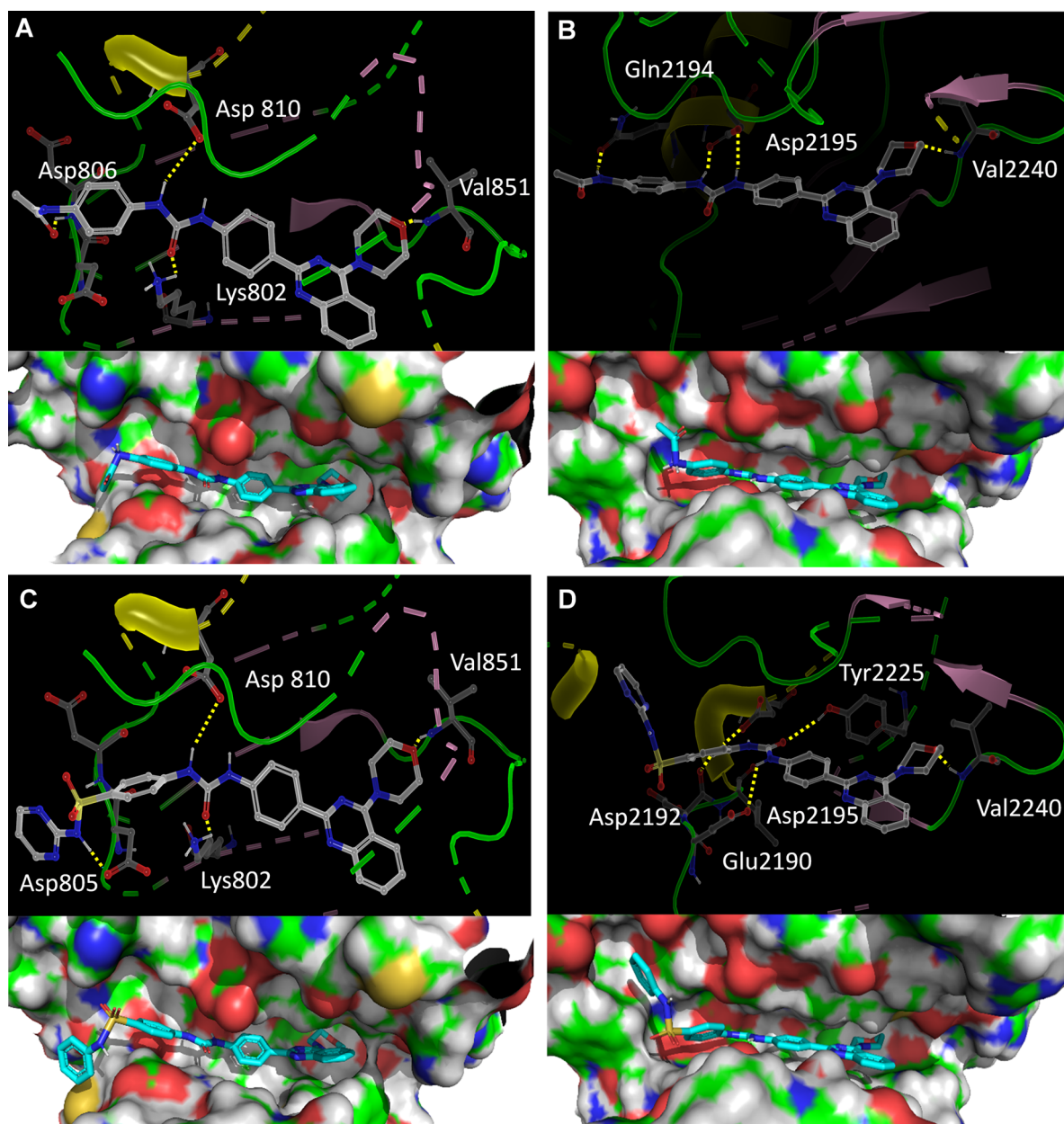


Figure 4. Docking of PI3K α -selective inhibitor **9k** and mTOR-selective inhibitor **9r** with the crystal structures of human PI3K α and mTOR showing hydrogen bonds and surface maps. (A) **9k** docked to PI3K α with four critical hydrogen bonds shown; (B) **9k** docked to mTOR with three critical hydrogen bonds shown; (C) **9r** docked to pI3K α with 4 critical hydrogen bonds shown; (D) **9r** docked to mTOR with 5 critical hydrogen bonds shown.

minimizations, to ensure that the morpholino groups of **9k** and **9r** were oriented similarly to the morpholino moiety of PI-103 in the binding pockets. The results are presented in Figure 4.

In agreement with results on our¹⁸ and other²¹ analogous pyrido-pyrimidines, our models indicated that both **9k** and **9r** retained the essential hydrogen bond between the morpholino oxygen and Val851 in the hinge region of PI3K α and Val2240 in the hinge region of mTOR. The hydrogen bonds predicted between the urea N–H groups and the aspartates in the hydrophobic binding pockets (Asp810 for PI3K α ; Asp2357 for mTOR) were also retained. One end of the binding pocket on PI3K α appears to be solvent-exposed, and a ridge of amino acid residues is present at the distal end of the binding pocket on mTOR that may make it more difficult for mTOR than for

PI3K α to accommodate larger residues as predicted from the SAR results.

The docking models do suggest reasons for the opposite selectivity seen with **9k** and **9r**. For **9k** (Figure 4A), two additional hydrogen bonding interactions are predicted (the acetamide -NH with Asp806 and the urea carbonyl oxygen with Lys802), while **9k** appears to form only one additional hydrogen bond with mTOR (the acetamide -NH with Gln2194) (Figure 4B). This could explain the selectivity for PI3K α over mTOR seen for **9k**. Alternatively, the mTOR-selective analog **9r** appears to make 5 hydrogen bonding interactions with mTOR (the three described above for **9k** plus two additional interactions between the urea carbonyl oxygen and Glu2190 and the sulfonamide -NH and Asp2192 (Figure 4D) as opposed to 4 hydrogen bonds formed with

PI3K α (the three described above for **9k** plus an interaction between the sulfonamide -NH and Asp805) (Figure 4C). This discrepancy may explain the selectivity for mTOR seen with **9r**. To confirm that our compounds act as dual PI3K α /mTOR inhibitors, we treated MCF7 cells with **9k** at concentrations of 62.5 and 125 nM for 4 h and then analyzed cell lysates for downstream targets of the two enzymes by Western blot. The results are shown in Figure 5. Compound **9k** dose-dependently inhibited the production of the PI3K α - and mTOR-associated signaling components phospho-4EBP, phospho-P70SK6, and phospho-AKT(473).

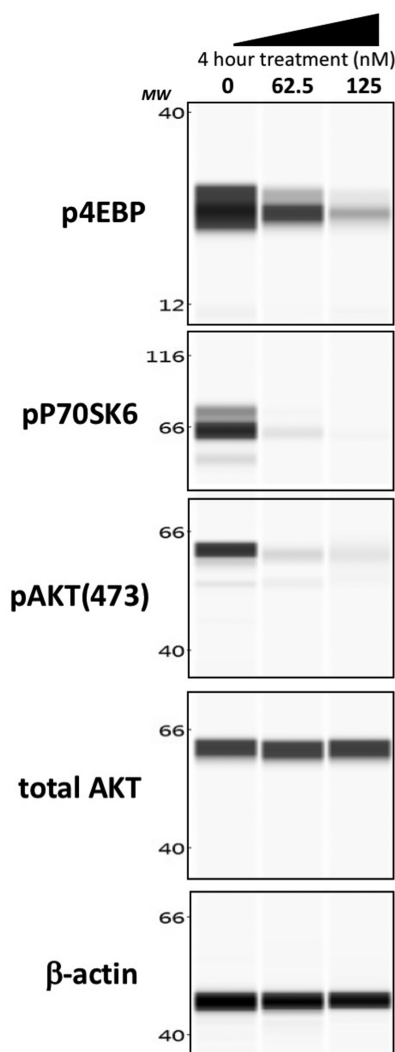


Figure 5. Western blot analysis of PI3K α and mTOR targets. Phosphorylation changes of phospho-4EBP, phospho-P70SK6, and phospho-AKT(473) in a dose-dependent treatment of MCF7 cells for 4 h with compound **9k**.

In vitro antitumor activity was initially evaluated by testing the effects of the more potent dual PI3K α /mTOR inhibitors on the cellular viability using a luminescent CellTiter-Glo assay (Promega, Madison, WI). Preliminary screening was carried out in 2D cell culture using a single 10 μ M concentration of selected analogs against three breast cancer cell lines (MDA-MB-468, MDA-MB-231, and MCF7). An approximation of therapeutic index was determined by screening the compounds

in normal human dermal fibroblasts. Results are provided in Table 3 as percent of viable cells.

Table 3. Percent of Cell Viability of 3 Breast Cancer Cell Lines and Normal Skin Cells in the Presence of 10 μ M Compounds as Tested by CellTiter-Glo[®]2D

Entry	Fibroblast	MDA-MB-231	MDA-MB-468	MCF7
9a	71	180	96	34
9b	95	146	65	31
9c	99	140	80	35
9d	88	138	56	21
9e	86	208	60	7
9f	94	138	47	13
9g	63	192	74	7
9h	20	74	42	22
9k	71	69	50	29
9l	80	66	54	12
9m	84	114	33	8
9n	38	137	66	8
9o	92	152	51	30
9p	95	140	59	40
PI 103	42	61	36	30
Untreated	100	100	100	100

Viability > 80%
Viability < 50%

The most prevalent effect on cancer cell viability by our compounds was seen in the estrogen-sensitive, HER2-negative MCF7 cell line. Four analogs, **9f**, **9h**, **9k**, and **9m**, also demonstrated reasonable cytotoxic activity against the triple negative cell line MDA-MD-468. Like the standard agent PI-103, none of our quinazoline derivatives showed appreciable cytotoxic activity in the claudin-low triple negative cell line MA-MDB-231 that could not be attributed to overt cellular toxicity. MDA-MB-231 cells are known to be less susceptible to chemotherapy.²² Several of the quinazoline analogs (**9b–f**, **9l–m**, **9o–p**) demonstrated a therapeutic index for MCF7 cells over normal cells that was superior to that seen with PI-103, and two derivatives (**9f**, **9m**) also demonstrated a therapeutic index for MDA-MB-468 cells over normal cells. These results are in contrast to the results obtained with the previously reported pyrido-pyrimidines,¹⁸ where only one analog possessed a therapeutic index for MCF7 over normal fibroblasts and none of the compounds demonstrated a therapeutic index for cytotoxicity in the triple negative cell lines over fibroblasts.

Compounds that displayed >50% cytotoxicity in MCF7 cells (shaded in red in Table 3) and >80% viability in dermal fibroblasts (shaded in green in Table 3) were examined for their cytotoxic effects on MCF7 cells in 3D cell culture using CellTiter-Glo 3D assay (Promega, Madison, WI). 3D cancer cell culture is believed to more accurately reflect *in vivo* tumor cell physiology and morphology as well as tumor architecture.²³ Dose response curves (Figure S1) were generated for

the most promising analogs (9b–g, 9l–m, 9o–p). We also examined compound 9k as the most potent PI3K α inhibitor and compound 9g as the most potent combined PI3K α /mTOR inhibitor. IC₅₀ values are given in Table 4.

Table 4. IC₅₀ Values for 9b–g, 9k, 9l–m, and 9o–p against MCF7 Cells in 3D Cell Culture (CellTiterGlo®3)

Cpd.	9b	9c	9d	9e	9f	9g
IC ₅₀ (μ M)	0.7	1.2	1.6	0.2	0.3	0.3
Cpd.	9k	9l	9m	9o	9p	
IC ₅₀ (μ M)	0.2	0.3	0.2	0.3	1.8	

All of the analogs tested displayed potent cytotoxic activity against MCF7 cells in 3D culture, with IC₅₀ values ranging from 0.2 μ M to 1.8 μ M. In general, IC₅₀ values were in agreement with the percent cytotoxic activity seen in the 2D assay (Table 3). The exceptions to this were 9c, 9d, and 9p which demonstrated IC₅₀ values that were higher than those obtained with the other analogs. The reasons for this are not clear at this point. These compounds displayed somewhat higher IC₅₀ values against mTOR activity compared to other analogs. However, other compounds with similar mTOR inhibitory potency (e.g., 9f) were found to be potent cytotoxic agents in the 3D cell culture model. One contributing factor may be solubility limitations. The compounds with higher than expected IC₅₀ values in the 3D culture model seemed to hit a ceiling effect (~30% viability) at the 7.5 μ M concentration, with no further effect seen at 15 μ M. Permeability in the 3D system could also have played a role. While the logP values for all tested analogs are within a range predicted to impart reasonable cellular permeability (2.0–4.6),^{24,25} the logP values of 9c (2.03), 9d (3.94), and 9p (4.37) fall near the outer limits of that range.

Since PI3K α and mTOR both possess serine/threonine kinase (STK) activity, we assessed the selectivity of compound 9k within the STK class of kinases in MCF7 cells using Pamgene's proprietary Pamchip microarray-based peptide activity profile (Pamgene International, B.V., s'Hertogenbosch, The Netherlands). The PamChip arrays generate relative phosphorylation intensity data of peptides containing known substrate recognition sites of STKs in the presence compound 9k and DMSO control. Using a differential upstream kinase analysis of bait peptides, we predicted top STKs (n = 20) whose activity was significantly inhibited by compound 9k at the 1 μ M concentration (1,300-fold higher than the IC₅₀ for PI3K α inhibition; 10-fold higher than the IC₅₀ for mTOR inhibition) in comparison to DMSO control as shown in Figure 6. The STK profile confirmed the PI3K α and mTOR inhibitory activity of 9k by demonstrating a decrease in levels of phospho-P70S6K and phospho-NAUK1 (downstream targets of mTOR) as well as phospho-AKTs (downstream targets of PI3K α). In addition, the STK profile demonstrated the inhibitory effect of compound 9k on kinases activity associated with the RAS, ErbB, and MAPK signaling pathways. A list of effected kinases and downstream phosphorylated peptides is provided in the Supporting Information.

In conclusion, straightforward synthetic routes were used to synthesize novel disubstituted quinazolines as potent dual PI3K α /mTOR inhibitors that demonstrated superior therapeutic indices for cytotoxic activity against breast cancer cell lines compared to earlier pyrido-pyrimidine compounds.

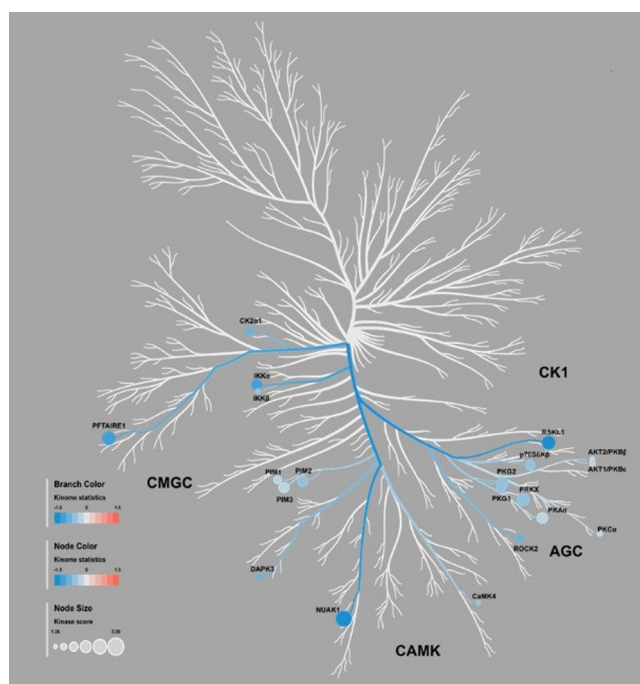


Figure 6. Kinome tree visualization of top predicted upstream serine/threonine kinases (STKs) where kinase statistics values, encoded in branch color and node color, indicate the overall change of the peptide set that represents the kinase, with value <0 indicating lower kinase activity in compound 9k (1 μ M) treated MCF7 cells relative to DMSO control. Kinase scores, encoded in node size, are used for ranking kinases based on their significance and specificity in terms of the set of peptides used for the corresponding kinase.

Removal of the urea moiety within the scaffold yielded weak dual inhibitors. On the other hand, combining the urea group with different hydrogen bonding substituents resulted in potent inhibitors that displayed a range of selectivity for PI3K α and mTOR. Substitution of the phenylurea ring with short alkyl chains or 6-membered heteroaryl/aryl sulfonamides afforded analogs with selectivity toward mTOR over PI3K α . Alternatively, substituting the phenylurea ring with the acetamide moiety provided 9k, a potent inhibitor of PI3K α (IC₅₀ = 0.7 nM) with 154-fold selectivity for PI3K α over mTOR. The selectivity seen within this series could be explained by differences in the number of hydrogen bonding interactions made with the two enzymes as predicted by docking studies performed with the X-ray crystal structures of human PI3K α and mTOR. Nine derivatives demonstrated potent cytotoxic activity against MCF7 cells in 2D culture and a good therapeutic index as assessed in normal dermal fibroblasts. Two of these analogs also showed cytotoxic activity against the triple negative breast cancer cell line MDB-MA-468. Most of these analogs also displayed potent cytotoxic IC₅₀ values against MCF7 cells grown in 3D cell culture, with potency in this assay aligning with potency against PI3K α and logP values predicted to impart good cellular permeability. In addition, we identified a new substituent motif that imparted potent PI3K α and mTOR inhibitory potency to the morpholino-quinazoline scaffold, namely the sulfonamide, as exemplified by compound 9m. This substituent has not been reported previously for such compounds. Off-target kinase inhibitory activity for a representative compound (9k) included STKs within the RAS, ErbB, and MAPK signaling pathways. All of these STK inhibitory activities could be

contributing to the potent cytotoxicity seen with **9k** in MCF7 cell cultures. Based on pharmacological and *in vitro* ADME properties, compounds **9e**, **9f**, **9g**, **9k**, **9m**, and **9o** will be advanced to *in vivo* studies which will be the subject of future reports.

■ ASSOCIATED CONTENT

SI Supporting Information

The Supporting Information is available free of charge at <https://pubs.acs.org/doi/10.1021/acsmmedchemlett.0c00289>.

Synthetic procedures for compounds **2**, **6**, **7a–e**, **8a–g**, and **9a–u**, biological methods, *in vitro* ADME procedures, and molecular modeling methods (PDF)

■ AUTHOR INFORMATION

Corresponding Authors

Aisha A. K. Al-Ashmawy – Moulder Center for Drug Discovery Research, Temple University, School of Pharmacy, Philadelphia, Pennsylvania 19140, United States; Department of Therapeutic Chemistry, Pharmaceutical and Drug Industries Research Division, National Research Center, Cairo 12622, Egypt; orcid.org/0000-0002-9219-5436; Phone: +201013231824; Email: Aisha_pharmacy@yahoo.com

Wayne E. Childers, Jr. – Moulder Center for Drug Discovery Research, Temple University, School of Pharmacy, Philadelphia, Pennsylvania 19140, United States; Phone: 215-707-1079; Email: wayne.childers@temple.edu

Authors

Khaled M. Elokely – Moulder Center for Drug Discovery Research, Temple University, School of Pharmacy, Philadelphia, Pennsylvania 19140, United States; Department of Pharmaceutical Chemistry, Tanta University, Tanta 31527, Egypt; Division of Pharmaceutical Sciences, Arnold and Marie Schwartz College of Pharmacy and Health Sciences, Long Island University, Brooklyn, New York 11201, United States

Oscar Perez-Leal – Moulder Center for Drug Discovery Research, Temple University, School of Pharmacy, Philadelphia, Pennsylvania 19140, United States

Mario Rico – Moulder Center for Drug Discovery Research, Temple University, School of Pharmacy, Philadelphia, Pennsylvania 19140, United States

John Gordon – Moulder Center for Drug Discovery Research, Temple University, School of Pharmacy, Philadelphia, Pennsylvania 19140, United States

George Mateo – Moulder Center for Drug Discovery Research, Temple University, School of Pharmacy, Philadelphia, Pennsylvania 19140, United States

Abdelsattar M. Omar – Department of Pharmaceutical Chemistry, Faculty of Pharmacy, King Abdulaziz University, Jeddah 21589, Saudi Arabia; Department of Pharmaceutical Chemistry, Faculty of Pharmacy, Al-Azhar University, Cairo 11884, Egypt; orcid.org/0000-0002-9825-3465

Magid Abou-Gharbia – Moulder Center for Drug Discovery Research, Temple University, School of Pharmacy, Philadelphia, Pennsylvania 19140, United States; orcid.org/0000-0001-7524-6011

Complete contact information is available at: <https://pubs.acs.org/10.1021/acsmmedchemlett.0c00289>

Author Contributions

The main idea, all of the chemistry work, and writing the manuscript was done by Aisha Al-Ashmawy. Docking study was carried by KE. OP and MR carried out the *in vitro* antitumor activity and Western blot. JG carried out *in vitro* ADME assays. GM carried out the HRMS. AO initiated the kinome screening assay. WC and MA helped in the editing and writing of the manuscript. All authors have given approval to the final version of the manuscript.

Funding

Funding was provided by The Egyptian Ministry of Higher Education/Central Department of missions (CDM) and United States Agency for International Development (USAID) and by Deanship of Scientific Research (DSR) at King Abdulaziz University, Jeddah under grant no. FP-61-42 for funding the kinome screening assay.

Notes

The authors declare no competing financial interest.

■ ACKNOWLEDGMENTS

The authors extend their appreciation for the Egyptian Ministry of Higher Education for sponsoring Aisha Al-Ashmawy as visiting scholar in addition to the United States Agency for International Development (USAID) for sponsoring Aisha Al-Ashmawy as postdoctoral fellow (GSP-P-75) for completion of the work. The authors acknowledge, with thanks, the DSR for technical and financial support. The authors thank Reaction Biology Corporation (Malvern, PA) for running *in vitro* kinase assays. The authors also thank Pamgene International B.V., especially Tushar Tomar and Dirk Pijnenburg, for providing the kinome screening data.

■ ABBREVIATIONS

PI3Ks, phosphatidylinositol-3-kinases; PIP2, phosphatidylinositol(4,5)-biphosphate; PIP3, phosphatidylinositol(3,4,5)-triphosphate; Akt, protein kinase B; mTOR, mammalian target of rapamycin; PIKKs, phosphoinositide-3-kinase related protein kinases; PI3KCA, phosphatidylinositol-4,5-bisphosphate 3-kinase catalytic subunit alpha; PTENS, phosphatase and tensin homologue deleted on chromosome ten; RTKs, receptor tyrosine kinases; 4EBP1, factor 4E-binding protein1; DME, dimethoxyethane; DMA, dimethylacetamide; DIPEA, N,N-diisopropylethylamine; ADME, absorption, distribution metabolism, and excretion; PDB, Protein Data Bank; STK, serine/threonine kinase.

■ REFERENCES

- (1) Sawyers, C. L.; Vivanco, I. The Phosphatidylinositol 3-Kinase-AKT Pathway in Human Cancer. *Nat. Rev. Cancer* **2002**, *2*, 489–501.
- (2) Maehama, T.; Dixon, J. E. The Tumor Suppressor, PTEN/MMAC1, Dephosphorylates the Lipid Second Messenger, Phosphatidylinositol 3,4,5-Trisphosphate. *J. Biol. Chem.* **1998**, *273* (22), 13375–13378.
- (3) Yap, T. A.; Garrett, M. D.; Walton, M. I.; Raynaud, F.; de Bono, J. S.; Workman, P. Targeting the PI3K-AKT-MTOR Pathway: Progress, Pitfalls, and Promises. *Curr. Opin. Pharmacol.* **2008**, *8*, 393–412.
- (4) Samuels, Y.; Ericson, K. Oncogenic PI3K and Its Role in Cancer. *Curr. Opin. Oncol.* **2006**, *18*, 77–82.
- (5) Campbell, I. G.; Russell, S. E.; Choong, D. Y. H.; Montgomery, K. G.; Ciavarella, M. L.; Hooi, C. S. F.; Cristiano, B. E.; Pearson, R.

- B.; Phillips, W. A. Mutation of the PIK3CA Gene in Ovarian and Breast Cancer. *Cancer Res.* **2004**, *64* (21), 7678–7681.
- (6) Dey, N.; De, P.; Leyland-Jones, B. PI3K-AKT-MTOR Inhibitors in Breast Cancers: From Tumor Cell Signaling to Clinical Trials. *Pharmacol. Ther.* **2017**, *175*, 91–106.
- (7) Zhao, W.; Qiu, Y.; Kong, D. Class I Phosphatidylinositol 3-Kinase Inhibitors for Cancer Therapy. *Acta Pharm. Sin. B* **2017**, *7*, 27–37.
- (8) Elmenier, F. M.; Lasheen, D. S.; Abouzid, K. A. M. Phosphatidylinositol 3 Kinase (PI3K) Inhibitors as New Weapon to Combat Cancer. *Eur. J. Med. Chem.* **2019**, *183*, 111718.
- (9) Akinleye, A.; Avvaru, P.; Furqan, M.; Song, Y.; Liu, D. Phosphatidylinositol 3-Kinase (PI3K) Inhibitors as Cancer Therapeutics. *J. Hematol. Oncol.* November 22, **2013**; pp 1–17. .
- (10) Courtney, K. D.; Corcoran, R. B.; Engelman, J. A. The PI3K Pathway as Drug Target in Human Cancer. *J. Clin. Oncol.* February 20, **2010**; pp 1075–1083. .
- (11) Venkatesan, A. M.; Dehnhardt, C. M.; Delos Santos, E. D.; Chen, Z.; Dos Santos, O. D.; Ayrak-Kaloustian, S.; Khafizova, G.; Brooijmans, N.; Mallon, R.; Hollander, I.; Feldberg, L.; Lucas, J.; Yu, K.; Gibbons, J.; Abraham, R. T.; Chaudhary, I.; Mansour, T. S. Bis(Morpholino-1,3,5-Triazine) Derivatives: Potent Adenosine 5'-Triphosphate Competitive Phosphatidylinositol-3-Kinase/Mammalian Target of Rapamycin Inhibitors: Discovery of Compound 26 (PKI-587), a Highly Efficacious Dual Inhibitor. *J. Med. Chem.* **2010**, *53* (6), 2636–2645.
- (12) Foster, P.; Yamaguchi, K.; Hsu, P. P.; Qian, F.; Du, X.; Wu, J.; Won, K. A.; Yu, P.; Jaeger, C. T.; Zhang, W.; Marlowe, C. K.; Keast, P.; Abulafia, W.; Chen, J.; Young, J.; Plonowski, A.; Yakes, F. M.; Chu, F.; Engell, K.; Bentzien, F.; Lam, S. T.; Dale, S.; Yturralde, O.; Matthews, D. J.; Lamb, P.; Laird, A. D. The Selective PI3K Inhibitor XL147 (SAR245408) Inhibits Tumor Growth and Survival and Potentiates the Activity of Chemotherapeutic Agents in Preclinical Tumor Models. *Mol. Cancer Ther.* **2015**, *14* (4), 931–940.
- (13) Papadopoulos, K. P.; Egile, C.; Ruiz-Soto, R.; Jiang, J.; Shi, W.; Bentzien, F.; Rasco, D.; Abrisqueta, P.; Vose, J. M.; Taberero, J. Efficacy, Safety, Pharmacokinetics and Pharmacodynamics of SAR245409 (Voxtalisis, XL765), an Orally Administered Phosphoinositide 3-Kinase/Mammalian Target of Rapamycin Inhibitor: A Phase 1 Expansion Cohort in Patients with Relapsed or Refractory Lymphoma. *Leuk. Lymphoma* **2015**, *56* (6), 1763–1770.
- (14) Hayakawa, M.; Kaizawa, H.; Moritomo, H.; Koizumi, T.; Ohishi, T.; Okada, M.; Ohta, M.; Tsukamoto, S.; Parker, P.; Workman, P.; Waterfield, M. Synthesis and Biological Evaluation of 4-Morpholino-2-Phenylquinazolines and Related Derivatives as Novel PI3 Kinase P110 Alpha Inhibitors. *Bioorg. Med. Chem.* **2006**, *14*, 6847–6858.
- (15) Raynaud, F. I.; Eccles, S.; Clarke, P. A.; Hayes, A.; Nutley, B.; Alix, S.; Henley, A.; Di-Stefano, F.; Ahmad, Z.; Guillard, S.; Bjerke, L. M.; Kelland, L.; Valenti, M.; Patterson, L.; Gowan, S.; Brandon, A. D. H.; Hayakawa, M.; Kaizawa, H.; Koizumi, T.; Ohishi, T.; Patel, S.; Saghir, N.; Parker, P.; Waterfield, M.; Workman, P. Pharmacologic Characterization of a Potent Inhibitor of Class I Phosphatidylinositide 3-Kinases. *Cancer Res.* **2007**, *67* (12), 5840–5850.
- (16) Peng, W.; Tu, Z. C.; Long, Z. J.; Liu, Q.; Lu, G. Discovery of 2-(2-Aminopyrimidin-5-Yl)-4-Morpholino-N-(Pyridin-3-Yl)Quinazolin-7-Amines as Novel PI3K/MTOR Inhibitors and Anticancer Agents. *Eur. J. Med. Chem.* **2016**, *108*, 644–654.
- (17) André, F.; Ciruelos, E.; Rubovszky, G.; Campone, M.; Loibl, S.; Rugo, H. S.; Iwata, H.; Conte, P.; Mayer, I. A.; Kaufman, B.; Yamashita, T.; Lu, Y. S.; Inoue, K.; Takahashi, M.; Pápai, Z.; Longin, A. S.; Mills, D.; Wilke, C.; Hirawat, S.; Juric, D. Alpelisib for PIK3CA-Mutated, Hormone Receptor-Positive Advanced Breast Cancer. *N. Engl. J. Med.* **2019**, *380* (20), 1929–1940.
- (18) Al-Ashmawy, A. A. K.; Ragab, F. A.; Elokely, K. M.; Anwar, M. M.; Perez-Leal, O.; Rico, M. C.; Gordon, J.; Bichenkov, E.; Mateo, G.; Kassem, E. M. M.; Hegazy, G. H.; Abou-Gharbia, M.; Childers, W. Design, Synthesis and SAR of New-Di-Substituted Pyridopyrimidines as ATP-Competitive Dual PI3K α /MTOR Inhibitors. *Bioorg. Med. Chem. Lett.* **2017**, *27* (14), 3117–3122.
- (19) Zhao, Y.; Zhang, X.; Chen, Y.; Lu, S.; Peng, Y.; Wang, X.; Guo, C.; Zhou, A.; Zhang, J.; Luo, Y.; Shen, Q.; Ding, J.; Meng, L.; Zhang, J. Crystal Structures of PI3K α Complexed with PI103 and Its Derivatives: New Directions for Inhibitors Design. *ACS Med. Chem. Lett.* **2014**, *5* (2), 138–142.
- (20) Yang, H.; Rudge, D. G.; Koos, J. D.; Vaidialingam, B.; Yang, H. J.; Pavletich, N. P. MTOR Kinase Structure, Mechanism and Regulation. *Nature* **2013**, *497* (7448), 217–223.
- (21) Saurat, T.; Buron, F.; Rodrigues, N.; De Tauzia, M. L.; Colliandre, L.; Bourg, S.; Bonnet, P.; Guillaumet, G.; Akssira, M.; Corlu, A.; Guillouzo, C.; Berthier, P.; Rio, P.; Jourdan, M. L.; Bénédicti, H.; Routier, S. Design, Synthesis, and Biological Activity of Pyridopyrimidine Scaffolds as Novel PI3K/MTOR Dual Inhibitors. *J. Med. Chem.* **2014**, *57* (3), 613–631.
- (22) Holliday, D. L.; Speirs, V. Choosing the Right Cell Line for Breast Cancer Research. *Breast Cancer Res.* August 12, **2011**; p 215. .
- (23) Edmondson, R.; Broglio, J. J.; Adcock, A. F.; Yang, L. Three-Dimensional Cell Culture Systems and Their Applications in Drug Discovery and Cell-Based Biosensors. *Assay and Drug Development Technologies*; Mary Ann Liebert Inc., May 1, 2014; pp 207–218. DOI: 10.1089/adt.2014.573.
- (24) Liu, X.; Testa, B.; Fahr, A. *Lipophilicity and Its Relationship with Passive Drug Permeation*; Pharmaceutical Research, May 2011; pp 962–977. DOI: 10.1007/s11095-010-0303-7.
- (25) Refsgaard, H. H. F.; Jensen, B. F.; Brockhoff, P. B.; Padkjær, S. B.; Guldbrandt, M.; Christensen, M. S. In Silico Prediction of Membrane Permeability from Calculated Molecular Parameters. *J. Med. Chem.* **2005**, *48* (3), 805–811.